Spin Dynamics in Strongly Correlated Electron Compounds

Yasuo Endoh

Department of Physics, Graduate School of Science, Tohoku University,

Aramaki Aza Aoba, Aoba-ku, Sendai, 980-77, Japan

Abstract

The recent neutron magnetic scattering results from strongly correlated electron compounds are reviewed. We have elucidated the spin fluctuations in the $3d$ transition metal oxides including the high temperature superconductors, the colossal magneto-resistance materials and related compounds. One important conclusion obtained from our studies is that spin dynamics or thermal spin fluctuations in these correlated electron systems are quite similar to those characterising itinerant electron magnetism.

1 Introduction

In the past decade, we have been interested in the physics of strongly correlated electron systems as the most fascinating subject in modern condensed matter physics. Materials of the strongly correlated electron systems commonly show unconventional properties as the result of nonlinear many-body electron forces plus various competing interactions acting on not only electrons and spins but also phonons. Among these we focus on transition metal oxides presented in this paper, which belong to the family of either a cubic perovskite of ABO_3, with A = Alkaline (-earth) metal cation, B = transition metal cation or their modified lattices.

The cubic perovskite of high symmetry is well known for its structural instabilities and it exhibits the distorted lower symmetry structure coupled with other freedoms such as electrons, (pseudo-)spins etc. (Samuelsen et al., 1972). Eventually it has become the important class of the 'strongly correlated materials' for not only the research of solid state physics but industrial application. The colossal magneto-resistance system of $La_{1-x}Sr_xMnO_3$ can be included in this category. On the other hand, the high T_c superconductors of the single layered copper oxide, $La_{2-x}Sr_xCuO_4$, have an A_2BO_4 unit lattice, where units of A_2O_2 plus BO_2 layers stack alternately. Therefore the lattice structure is quasi two dimensional (2D),

and in fact the physical properties are of mostly 2D character.

Another important aspect of these transition metal oxides presented here is the 'Mott transition' upon doping charges (holes) into the parent material. The insulating state is realized by the effect of the strong electron correlation. In other words, the half-filled band is split by the electron correlations and then the lower split band becomes fully occupied, hence an insulator. The insulating state of this category exhibits the antiferromagnetic long-range order due to the strong electron correlation. La_2CuO_4 and $LaMnO_3$ are both considered to be realizations of the Mott insulator or Mott–Hubbard insulator (Hubbard, 1963; Kanamori, 1963; Gutzwiller, 1963).

Spin fluctuations in the strongly correlated electron systems have become a central issue for the mechanism of the high T_c superconductivity: how strong the 2D antiferromagnetic interaction governs the metallic state of these high T_c superconducting copper oxides, which might be extended from the 2D quantum antiferromagnetism in the insulating state of La_2CuO_4. Furthermore it must be clarified experimentally how the unique spin fluctuations play a key role in the mechanism of the unconventional superconductivity.

Among many recently discovered high T_c superconductors of the copper oxides, the single layered copper oxide materials of $La_{2-x}Sr_xCuO_4$ have been focussed on in our group mainly due to the fact that this system is the simplest material among the high T_c superconductors and also the fact that undoped La_2CuO_4 ($x = 0$) is the most ideal 2D quantum ($S = 1/2$) Heisenberg antiferromagnet in our long standing interest. The main stream of our research activities for a decade have been summarized in several review papers (Birgeneau and Shirane, 1989; Endoh, 1990; Shirane et al., 1994). Therefore the first half of this paper deals with the most recent progress in our investigation of spin fluctuations in the superconducting phase of $La_{2-x}Sr_xCuO_4$ with $x = 0.15$, which gives the highest transition temperature ($T_c = 37.3$ K) in this particular system of the single layered superconductors. We also present the doping (x) dependence of the wave vector (δ) of the incommensurate spin fluctuations in the following section.

In the latter half, we discuss spin dynamics in the colossal magneto-resistance materials of $La_{1-x}Sr_xMnO_3$, with $x < 0.3$ (Martin et al., 1996). Spin correlations were predicted to be unusual reflecting the colossal magneto-resistance effect, which is the gigantic jump in resistivity associated with the long range magnetic order. The transition from the antiferromagnetic insulator to ferromagnetic metal at around $x \approx 0.15$ is induced by the double exchange interaction due to the spin canting (de Gennes, 1960). A dimensional crossover behaviour in $La_{1-x}Sr_xMnO_3$ at around $x \approx 0.1$ (Hirota et al., 1996) will also be interpreted by the double exchange interaction. Finally we will show that the characteristics of spin dynamics in the metallic phase of $La_{1-x}Sr_xMnO_3$ can be mapped onto the ferromagnetic
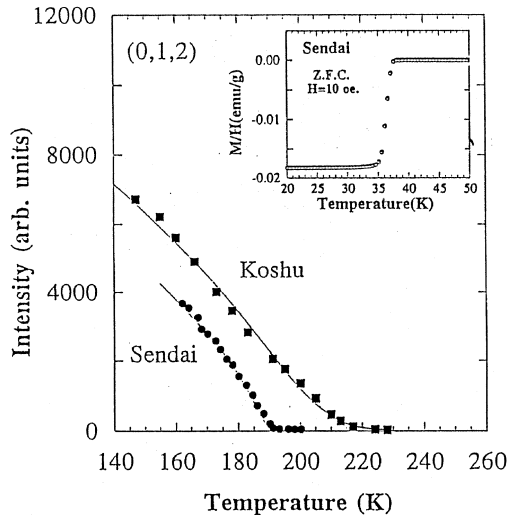
Figure 1. Temperature dependence of peak intensities of (0,1,2) superlattice reflection near and below the structural phase transition of $La_{1.85}Sr_{0.15}CuO_4$ single crystals of 'Sendai' ($T_c = 37.3$ K) and 'Koshu' ($T_c = 33$ K). Insert is given the superconducting transition of Sendai crystal (Yamada et al., 1995).

transition metals, such as MnSi (Ishikawa et al., 1985), Ni (Steinvoll et al., 1984), Fe (Wicksted et al., 1984), Pd_2MnSn (Shirane et al., 1985), EuO (Boni and Shirane, 1986) or recently studied CoS_2 (Hiraka, 1996).

Note that the neutron scattering results very much depend on the quality as well as the size of the single crystals, and naturally the single crystal growth is one of the most important research activities in our group. Most of the oxide crystals used for our neutron scattering experiments were grown by the Traveling Solvent Floating Zone (TSFZ) method using the lump-image focusing furnace (Hosoya et al., 1994). This method is very useful for the production of pure and large samples because any impurity can be excluded during the melting and the oxygen atmosphere can be readily controlled as desired. A typical size of the single crystal is 7 mm in diameter and 3–4 cm in length of each rod.

The homogeneity of the grown single crystal of $La_{2-x}Sr_xCuO_4$ was characterized by the sharpness of the tetragonal-orthorhombic structural phase transition as shown in Fig. 1 (Yamada et al., 1995). The temperature dependence of the peak intensities at $(0, 1, 2)$ (Bamb notation) superlattice is shown in our studies, which is proportional to the square of the orthorhombic order parameter. It is well known that the data are described by the rounded power laws of $(T'_t - T)^{2\beta}$,

where the structural phase transition temperature T_t' has a Gaussian distribution with the mean value T_t and a half width $\sigma_{1/2}$; β was held fixed at the 3D XY value of 0.35. $\sigma_{1/2}$ was determined to be 1.4 K and $dT_t/dx = -2600$ K. Thus the experimental result corresponding to an inhomogeneity was determined to be 6×10^{-4} in x. $T_c = 37.3$ K as well as the sharpness in ΔT_c prove the highest quality among existing single crystals used at least for neutron scattering studies. For instance, the other crystals used in the previous experiments show $T_c \approx 33$ K and the inhomogeneity of 4×10^{-3} in x (Matsuda et al., 1994).

The lower energy neutron scattering experiments have been carried out on the triple axis spectrometers of both TOPAN installed at the JRR3 in JAERI and H7 installed at the HFBR in BNL. The high energy time of flight (TOF) neutron scattering experiments have been also made on the chopper spectrometer installed at the pulsed spallation neutron source of ISIS in DRAL.

2 Dynamical susceptibility in superconducting La$_{2-x}$Sr$_x$CuO$_4$

2.1 Incommensurate spin fluctuations

Dynamical magnetic susceptibility in low energies, typically less than 20 meV in the superconducting La$_{2-x}$Sr$_x$CuO$_4$ is well characterized by the incommensurate spin fluctuations: sharp peaks appear at $Q_\delta = (\pi(1 \pm \delta), \pi)$ and $(\pi, \pi(1 \pm \delta))$ in the 2D reciprocal space of the square lattice representation (Matsuda et al., 1994; Mason et al., 1992). As shown in Fig. 2, the magnetic peaks which correspond to four rods extending along $[0, 0, L]$ intersect the $(H, K, 0)$ plane at Q_δ. First, we present the doping effect of the wave vector of the incommensurate spin fluctuations, i.e. x–δ relationship.

As mentioned earlier, the experimental data specifying a relation between spin correlations and/or fluctuations and electronic properties, such as the carrier densities of the doping holes, should be very sensitive to the crystal quality. Systematic experiments combining careful neutron scattering measurements with precise bulk measurements can only provide the reliable determination of the wave vector (δ) of the incommensurate spin fluctuations, the development of the spin correlations, chemical composition, the super-conducting temperature (T_c), and consequently x–δ. Since we must determine these values for the crystals of different x, we tried to keep the identical single-crystal growth condition of the TSFZ method and post-growth heat treatment, as well. We have also minimized possible errors in various stages of the experimental process. The experimental error was determined to be no more than 0.008 in nominal x, which is accurate enough for the present purpose.
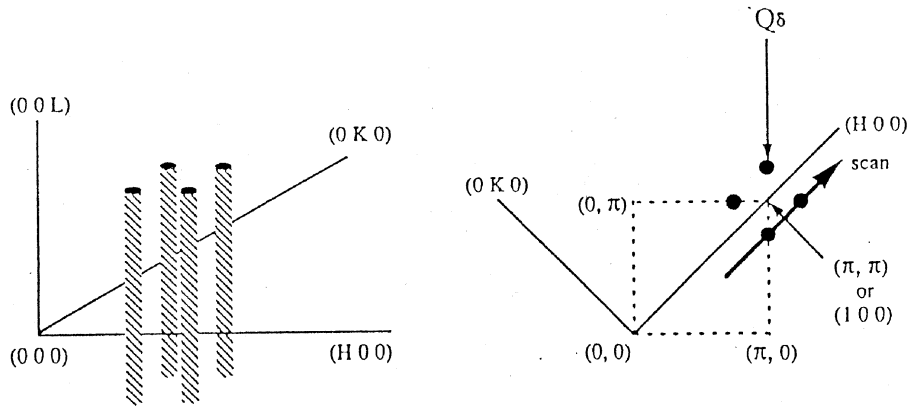
Figure 2. The schematic drawing of the 2D incommensurate spin fluctuations. 4 rods are located at $Q_\delta = (\pi, \pi(1 \pm \delta))$ and $(\pi(1 \pm \delta), \pi)$ in the c plane. δ is 0.24 rlu for $x = 0.15$.

The accuracy of δ is seen in the following figures (Yamada et al., 1996).

We have already presented a nonlinear x–δ relation (Endoh et al., 1992). We can now show unambiguously the nonlinearity, which is shown in Fig. 3. It must be emphasized here that the double peaked spectra become noticeable above $x = 0.05$, approximately corresponding to the superconducting phase boundary. Precisely speaking, x–δ is approximately linear in $x > 0.05$ with slight deviation downwards occurring beyond $x \approx 0.12$. Note that previous neutron scattering studies with the most recent result show the single peaked spectra centered at (π, π) at $x < 0.04$. We have also obtained a surprising result that δ is proportional to T_c in the latest investigation, which is presented in the same figure. We argue that this result should be a direct evidence of a causal relation of the superconductivity and incommensurate spin fluctuations in the single layered superconductors of the $La_{2-x}Sr_xCuO_4$ crystals.

As for the result of the incommensurate spin correlations in the superconducting state of the $La_{2-x}Sr_xCuO_4$ crystals, several models are proposed. The first model is the nesting of the large hole band at the Fermi energy (Si et al., 1993). The second is the possible existence of a stripe phase of doped holes with the periodic antiferromagnetic regions in between (Kievelson and Emery, 1996) and finally the third is the frustration of the Cu^{2+} spins caused by doped holes (Aharony et al., 1989), which eventually induces the periodic modulated spin structure. Related to the first model of the d–p band picture, the incommensurate spin fluctuations was
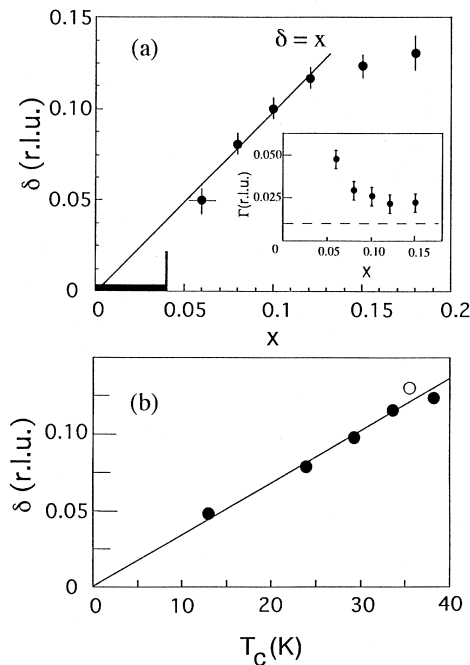
Figure 3. Incommensurability, δ plotted with respect to x in top. $\delta = 0$ for $x < 0.04$ is represented by thick line in the figure. The insert is the line width in q for $\omega = 2$ meV scan. The bottom panel shows the relationship between δ and the superconducting transition temperature, T_c (Yamada et al., 1996).

also predicted by the model started from the t-J model (Zhang and Rice, 1988). The d-band nature of $La_{2-x}Sr_xCuO_4$ is introduced and therefore it is defined as an extended t-J model (Fukuyama et al., 1994). Then an enhanced peak appears at the wave vectors, $Q_\delta = (\pi(1 \pm \delta), \pi)$ and $(\pi, \pi(1 \pm \delta))$, instead of (π, π) for the t-J model only. The relation of x–δ calculated by the extended t-J model quite resembles the experimental observation, except the δ which starts finite from $x = 0.1$ in calculation (Tanamoto, 1995). In the second model, the phase separation ascribes the competition between the long range Coulomb interaction and the broken exchange bond energy. This model became lively because of its successful interpretation of the charge ordering and modulated antiferromagnetic structure in the insulating phase of $(La_{0.6}Nd_{0.4})_{0.88}Sr_{0.12}CuO_4$ and La_2NiO_{4+y} (Tranquada et al., 1995). As far as we understand, δ in this model is mainly controlled by the concentration of the doped charge. In this respect, we observed that δ in the insulating La_2NiO_{4+y} or $La_{2-x}Sr_xNiO_4$ (Nakajima et al., 1996) is proportional to the doping

concentration of either y or x. Note that in these nickelate oxides, the charge ordering was confirmed experimentally together with the oxygen staging of the regular stacking along the crystalline c axis. On the other hand, there has been no detection of the moving domain walls in superconducting $La_{2-x}Sr_xCuO_4$. Therefore it seems to us very difficult to extend this phase separation model straightforwardly to the superconducting phase.

2.2   Hierarchical structure in spin dynamics in superconducting phase

The magnetic scattering at 4 K is buried in the experimental background, though the sharp peaks appear at Q_δ in the normal state above T_c as mentioned above (Yamada et al., 1995). We searched the careful temperature dependence of the scattering showing the exponential decay of the scattering intensity towards $\omega = 0$, and $T = 0$, and then we evaluated the energy gap, ω_c, in spin excitations to be 3.5 meV at $\delta = 0.24$ in the superconducting state, shown in Fig. 4. The superconducting gap energy, Δ_0 is estimated at 11 meV by the following equation proposed by the t-J model (Tanamoto et al., 1994)

$$\omega_c = \Delta_0 \sin(\pi\delta/2).$$

This evaluation also directly brings a conclusion for the long time issue concerning the symmetry of the superconducting wave function in a high T_c superconductors. The t-J model predicted that the unconventional superconductivity gives rise to the $d_{x^2-y^2}$ wave symmetry and the ratio of $2\Delta_0/T_c$ is about seven, which is consistent with the experimental results as well.

Let us proceed to another aspect of higher energy excitations which have been studied to comprehend the overall feature of the unique spin fluctuations in the superconducting state (Yamada et al., 1994). Our experimental data are essentially the same as are shown in the recent publication (Hayden et al., 1996), but the most recent data are much improved with a good signal to noise ratio. Magnetic excitations in the superconducting state well below T_c show that the strong 2D antiferromagnetic spin correlations in the undoped La_2CuO_4 (Hayden et al., 1992; Itoh et al., 1993) is not drastically renormalized by doping of holes even in the superconducting state. This phenomenon is expressed from a different point of view such that the low energy spin dynamics influenced by the conduction electrons of doped holes change to the dynamics of localized spins at Cu^{2+} sites in a higher energy range.

Unlike the magnetic excitation or $S(q,\omega)$ in $YBi_2Cu_3O_7$ (Fong et al., 1995), $La_{1.85}Sr_{0.15}CuO_4$ has a featureless spectra in which the broad peak centered at (π,π) extends to the cut-off energy of 280 meV. It must be noted that we can hardly

La$_{1.85}$Sr$_{0.15}$CuO$_4$ (T$_c$ = 37.3K)
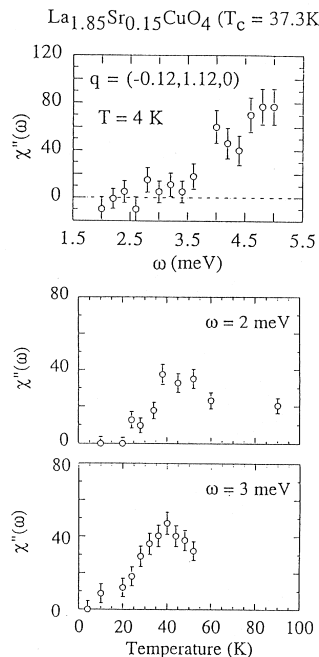
Figure 4. $\chi''(q = Q_\delta, \omega)$ is plotted as the function of transfer energy, ω at $T = 4$ K (top). Temperature dependence for $\omega = 2$ meV (middle), and 3 meV (bottom) are also shown (Yamada et al., 1995).

determine any specific structure in energy, though Hayden et al. (1996) claimed a shallow peak at around 20 meV in $\chi''(\omega)$. The cut off energy determined to be as high as 280 meV is essentially the same as the zone boundary energy of spin-wave excitation, just above 300 meV in La$_2$CuO$_4$ taking account of the considerable energy broadening in the doped crystal. We argue that we could define another type of crossover or a hierarchical structure in spin dynamics clarifying from the metallic character in the low energy to the localized one in high energy.

Related to this particular point, the qualitatively resembled magnetic excitation spectra have been observed in the Spin Density Wave (SDW) state of Cr at low temperatures well below the ordering temperature (T_N) (Endoh et al., 1994; Fukuda et al., 1996). In energies lower than about 15 meV, the sharp peaks appear at $Q = (\pi/a)(1 \pm q_{SDW}, 0, 0)$ where q_{SDW} is the SDW wave vector. In this case of the SDW, another peak centered at $Q = (1, 0, 0)$ of the antiferromagnetic reciprocal reflection takes over the incommensurate peaks at higher energies. (Fig. 5) The
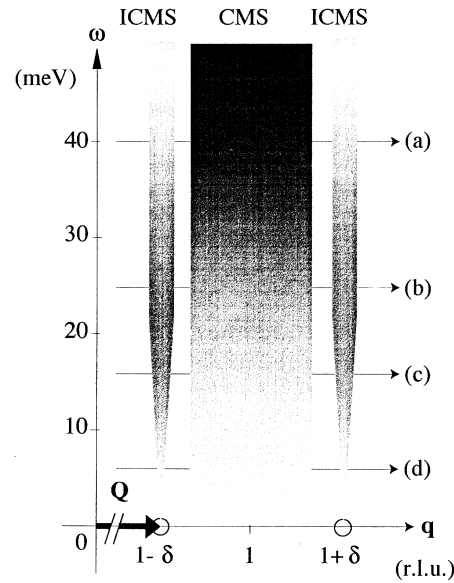
Figure 5. Schematic drawing of magnetic excitations from the SDW state in Cr. ICMS and CMS, respectively represent incommensurate and commensurate magnetic scattering. δ is the SDW wave vector in rlu unit.

magnetic excitations are still distinguishable from the background in very higher energies above 500 meV. Since the excitation energy goes up to eV regions, the cut off energy of the excitation could hardly be determined in the current experimental conditions. Although the phenomena are very much similar in two cases, the physics does not seem to be quite identical. In the present case of the high T_c superconductor, we look at the excitations from the magnetically disordered state. On the other hand, the magnetic excitation in Cr are from the ordered SDW. Usually any RPA calculation based on the two band model could predict spin wave mode which is presented by the linear dispersion relation of $w^{\pm} = A(q_{\text{SDW}} \pm q)$ from the SDW ordered state. In fact, the observed magnetic excitations are not so simple. As just mentioned above, the excitations have a triple peak structure. The energy spectra or $\chi''(\omega)$ of the SDW state in Cr gives a broad peak around 20 – 50 meV. Although we cannot find a reasonable interpretation, we can point out a remarkable similarity that both materials exhibit the sharp excitation peaks centered at the incommensurate wave vector dominates in lower energy and the single broad peak centered at the commensurate wave vector takes over as the excitation energy increases. The cut off energy is very large of the order of 1000 K or above

in both cases.

3   Spin dynamics in colossal magnetoresistance oxides

Tokura et al. (1995) first claimed that the colossal magnetoresistance phenomena in the metallic $La_{1-x}Sr_xMnO_3$ ($x < 0.3$) near below T_c should inherit the concept that the $LaMnO_3$ is the Mott–Hubbard insulator. Since then, this system became the important class of materials in the 'strongly correlated electron systems'. We have started neutron scattering experiments in order to elucidate the physical origin of the strange properties of the colossal magnetoresistance (CMR) from a view point of the strongly electron correlation effect, which should be active in the dynamical spin structure. It must be emphasized here that in a narrow range of x for $A_{1-x}M_xMnO_3$, where A = divalent alkaline metal cations, M = trivalent alkaline earth cations, there appear many complicated phase transitions. It should also be noted here that the classical neutron diffraction experiments studied by Wollan and Koehler (1955) from powdered samples of $La_{1-x}Sr_xMnO_3$ are still valuable, since all the complicated magnetic structures and lattice symmetries for the whole x range were determined. Nevertheless, mutual competing interactions among spins, charge and lattice as well as the change of the electron correlations upon doping of holes are naturally expected.

We understand well that the double exchange interaction leads to the transition from antiferromagnetic insulator to ferromagnetic metal upon doping of Sr (de Gennes, 1960), associated with increase of the spin canting. Furthermore the lattice structure at $x \approx 0.175$ shows a successive structural phase transition in thermal evolution, where the largest CMR effect is observed (Urushibara et al., 1995).

We first present here well defined spin-wave scattering in the ordered state of all the crystals of $La_{1-x}Sr_xMnO_3$ with $x = 0$, 0.05, 0.12, 0.2 and 0.3. The spin-wave dispersion in the antiferromagnetic phase of $LaMnO_3$ ($x = 0$) is very anisotropic as shown in Fig. 6 (Hirota et al., 1996). It is like a 2D dispersion relation; a typical ferromagnetic curve in the ($H\,K\,0$) plane in the orthorhombic notation. The zone boundary energy is larger than the energy corresponding to $T_N = 140$ K. On the other hand, the observed dispersion curve along $[0\,0\,L]$ is a typical antiferromagnetic spin-wave dispersion relation with a remarkably lower zone boundary energy than the other. This anisotropic spin-wave dispersion reflects the order parameter of the staggered magnetization near below T_N. The critical index of the order parameter, β is about 0.2, which is far smaller than any of those of 3D antiferromagnets. Therefore $LaMnO_3$ is considered to be a quasi 2D antiferromagnet; the 2D ferromagnetic lattices stacking along the c axis antiferromagnetically. Note that
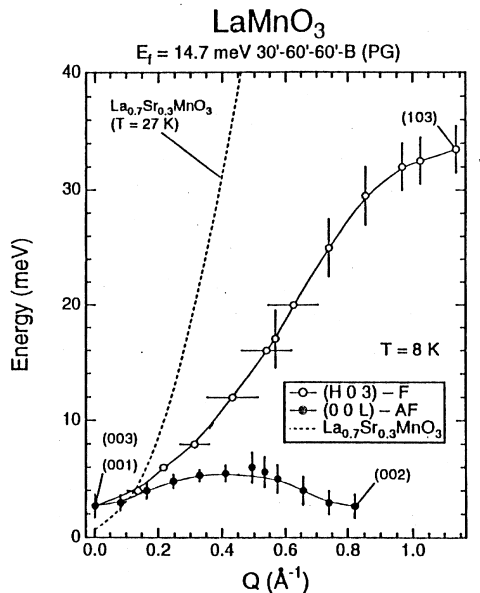
Figure 6. Spin-wave dispersion curves of LaMnO$_3$ along $(1\,0\,0)$ and $(0\,0\,1)$ directions (orthorhombic notation). The isotropic ferromagnetic spin-wave dispersion of La$_{0.7}$Sr$_{0.3}$MnO$_3$ is shown as the reference (Hirota et al., 1996).

the crystal structure is nearly isotropic with orthorhombic distortions as mentioned below. The 2D magnetic character should reflect the orbital order of $(3x^2 - r^2)$ and $(3y^2 - r^2)$ in the e_g band (Goodenough, 1955). Although the real lattice structure of LaMnO$_3$ is distorted to orthorhombic, Pbnm as the result of the Jahn-Teller effect, the orbital order itself as well as the 2D ferromagnetic character was predicted by Kanamori who considered extensively the superexchange mechanism in various $3d$ orbitals in the cubic crystalline field (Kanamori, 1959). It should be remarked that there is a considerable energy gap in the spin wave, about 2.5 meV at $q = 0$.

At elevated temperatures, only low energy spin excitations in small q are renormalized, as expected, leaving the higher energy part a little changed. This means that the antiferromagnetic order is controlled by $\sqrt{J'J}$, where J', interlayer exchange and J, intralayer exchange interaction. The strong intralayer magnetic interaction is the consequence of the squared ferromagnetic lattice with the 180° superexchange interaction. The magnetic excitations in $x = 0.05$ crystal are essentially similar to those of the undoped crystal, but the energy dispersion along the c axis is nearly constant; more complete 2D character.

On the contrary, we found the very isotropic 3D ferromagnetic spin-wave dis-

La$_{1-x}$Sr$_x$MnO$_3$
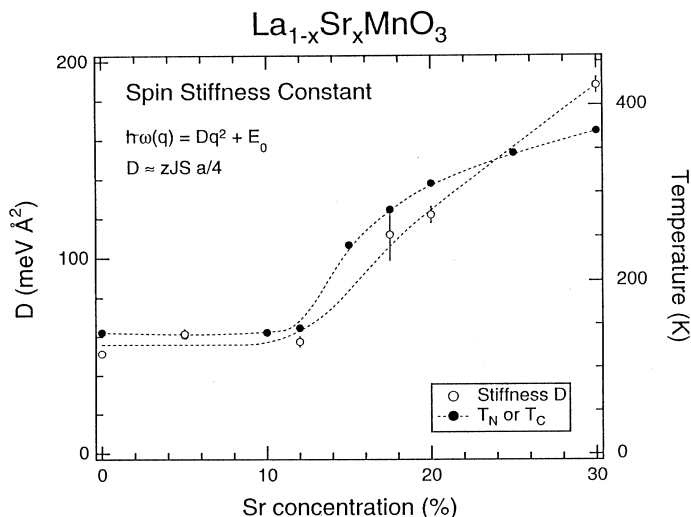
Figure 7. Spin-wave stiffness constant, D and the magnetic transition temperature (T_N or T_c) are plotted with respect to doping concentration of Sr.

persion curve when x reaches approximately 0.1. The zone boundary energies are beyond the experimental condition of the triple axis spectroscopy with thermal neutrons, but the exchange integral could be well estimated from the lower part of spin-wave dispersion or spin-wave stiffness constant D, which was reproduced by the motion of equation in terms of the model Heisenberg Hamiltonian with nearest neighbour exchange only. An important finding here is the fact that the exchange integral or the nearest neighbour interaction increases steadily with x, which almost coincides with the change in T_c as the function of x (Fig. 7).

The 2D ferromagnetic feature characterized the magnetism of the insulating LaMnO$_3$ reflects the orbital order of $3x^2 - r^2$ and $3y^2 - r^2$ in e_g band. Therefore this gives rise to the evidence of the orbital order and furthermore that the crossover effect becomes evident from the 2D ferromagnetic feature to 3D ferromagnetic character of metallic phase, besides the antiferro- to ferromagnetic transition. We remark that this magnetic transition occurs at $0.05 < x < 0.1$, where the conductivity still behaves like the semiconductor or insulator. This means that the metallic feature in spin dynamics is already visible below the lower doping level than the actual metal-insulator transition appears.

Paramagnetic scattering in small q region which has a double Lorentzian func-
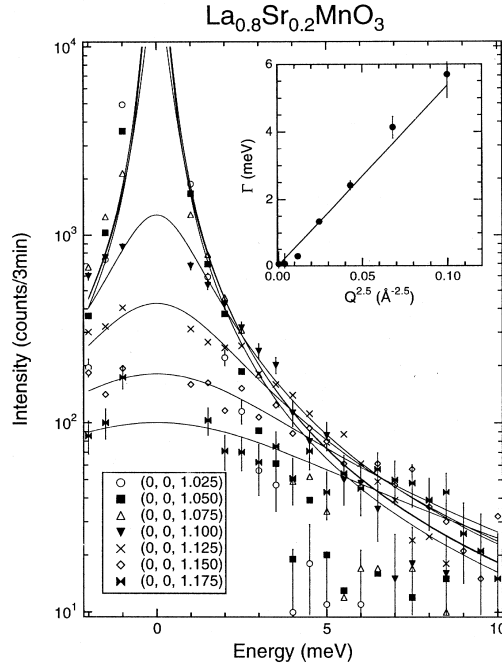
Figure 8. Lorentzian fitting of the magnetic critical scattering in $La_{0.8}Sr_{0.2}MnO_3$.

tion with respect to energy and momentum is represented as follows,

$$
\begin{aligned}
S(q,\omega) &\propto \frac{\hbar\omega/kT}{1-\exp(-\hbar\omega/kT)} kT\chi(0) \frac{\kappa_1^2}{\kappa_1^2+q^2} \cdot \frac{\Gamma}{\Gamma^2+\omega^2} \\
\kappa_1 &= \kappa_0(1-T/T_c)^{-\nu} \\
\Gamma &= Aq^{2.5}\left\{1+(\kappa_1/q)^2\right\}
\end{aligned}
$$

where A and κ_0 characterize the dynamical feature. As shown in Fig. 8, the analysis by introducing the double Lorentzian functional form is reasonable and in particular A was determined by the theoretical result of the critical scattering from the Heisenberg ferromagnet (Marshall and Lovesey, 1971). The scattering intensity contour presents a characteristic feature of $\chi''(q,\omega)$ in the Heisenberg ferromagnets. We emphasize here that the paramagnetic scattering just above T_c in the most of typical transition metal ferromagnets like Fe, Ni, Pd_2MnSn, EuO, MnSi or even recently observed CoS_2 obeys the double Lorentzian shape, and importantly the intensity contour map observed in the ferromagnets becomes quite universal when the map is scaled by these two characteristic parameters of A and κ_0. The result

of the scaling analysis is shown in the Table I. From the accumulated values of ratio of T_C^{MF}/T_C (T_C^{MF} = mean field Curie temperature) and A/T_C or D/T_C we just phenomenologically argue that these ratios represent a degree of the electron correlations. Stronger the electron correlation, the smaller the ratio, approaching unity as is expected. Inversely, when the kinetic energy or transfer energy is large, consequently the ratio becomes large. The important points addressed here is that the ratio of metallic $La_{1-x}Sr_xMnO_3$ is the same as that of Fe, as shown in Table I. Then if we define the metallic $La_{1-x}Sr_xMnO_3$ as the strongly electron correlated system, how do we think the ferromagnetic nature in metallic Fe? Even it is very important the fact that almost all the metallic ferromagnets have the similar ratios with each other.

Table I. Various quantities characterizing the dynamical ferromagnetic properties in typical transition metals of EuO, Pd_2MnSn, Fe, CoS_2, MnSi and Ni compared with the ferromagnetic phases of $La_{1-x}Sr_xMnO_3$ ($x = 0.3$, and $x = 0.2$). A and A^* in the table were evaluated by the present author from the original papers. Note that d^* and A^* are, respectively, inverse nearest neighbour distance and reduced value of A with respect to d^*.

	T_C (K)	$D(0.8T_C)$ ($meV\mathring{A}^2$)	A ($meV\mathring{A}^{2.5}$)	d^* ($\mathring{A}^{-1}$)	A^*/T_C
EuO	69	7.4	8.3	2.1	0.77
Pd_2MnSn	190	70	60	1.7	1.2
Fe	1040	175	140	3.1	2.3
CoS_2	121	106	71	2.0	3.1
MnSi	30	50	20	1.9	3.3
Ni	631	330	330	3.1	9.4
$La_{0.7}Sr_{0.3}MnO_3$	378	114	≈ 70	2.9	≈ 2.7
$La_{0.8}Sr_{0.2}MnO_3$	316	89	54	2.9	2.5

Finally, as far as spin dynamics is concerned, the spin dynamics in metallic $La_{1-x}Sr_xMnO_3$ is quite normal in all temperature range we have studied. Concomitantly there is no clear evidence that phonon softening occrs in the vicinity of the magnetic phase transition. It should be noted that the lattice distortion from the cubic perovskite to either rhombohedral or orthorhombic symmetry is far larger than the typical (anti-)ferroelectric perovskites like $SrTiO_3$ (Shirane, 1959). Since the specific mechanism of the colossal magnetoresistance is not fully understood yet, in particular the relation or the interplay among electron (charge), orbital

(electron-phonon coupling) and spins, further experimental explorations must be very important.

Acknowledgements

References

Aharony A, Birgeneau RJ, Coniglio A, Kastner MA and Stanley HE, 1988: Phys. Rev. Lett. **60**, 1330

Birgeneau RJ and Shirane G, 1989: *Physical Properties of High temperature Superconductors*, ed. by D.M. Ginzburg (World Scientific, Singapore) p. 151

Boni P and Shirane G, 1986: Phys. Rev. B **33**, 3012

de Gennes PG, 1960: Phys. Rev. **118**, 141

Endoh Y, 1989: Phase Transitions **15**, 223

Endoh Y, Yamada K, Matsuda M, Nakajima K, Kuroda K, Hidaka Y, Tanaka I, Kojima H, Birgeneau RJ, Kastner MA, Keimer B, Shirane G and Thurston TR, 1992: Jap. J. Appl. Phys. **7**, 174

Endoh Y, Fukuda T, Yamada K and Takeda M, 1994: J. Phys. Soc. Jpn. **63**, 3572

Fong HF, Keimer B, Anderson PW, Reznik D, Dogan F and Aksay A, 1995: Phys. Rev. Lett. **75**, 316

Fukuda T, Endoh Y, Yamada K, Takeda M, Itoh S, Arai M and Otomo T, 1996: J. Phys. Soc. Jpn. **65**, 1418

Fukuyama H, Kohno H and Tanamoto T, 1994: J. Low. Temp. Phys. **95**, 309

Goodenough JB, 1955: Phys. Rev. **100**, 564

Gutzwiller MC, 1963: Phys. Rev. Lett. **10**, 159

Hayden SM, Aeppli G, Mook HA, Cheong SM and Fisk Z, 1990: Phys. Rev. B **40**, 10220

Hayden SM, Aeppli G, Mook HA, Perring TG, Mason TM, Cheong SM and Fisk Z, 1996: Phys. Rev. Lett. **76**, 1344

Hiraka H, 1996: Thesis (Tohoku Univ.)

Hirota K, Kaneko N, Nishizawa A and Endoh Y, 1996: J. Phys. Soc. Jpn. **65**, Dec. issue

Hosoya S, Lee CH, Wakimoto S, Yamada K and Endoh Y, 1994: Physica C **235-240**, 547

Hubbard J, 1963: Proc. Roy. Soc. **A276**, 238

Ishikawa Y, Noda Y, Uemura, YJ, Majkrzak CF and Shirane G, 1985: Phys. Rev. B **31**, 5884

Itoh S, Yamada K, Arai M, Endoh Y, Hidaka Y and Hosoya S, 1994: J. Phys. Soc. Jpn. **63**, 4542

Kanamori J, 1959: J. Phys. Chem. Solids **10**, 87

Kanamori J, 1963: Prog. Theor. Phys. **30**, 275

Kievelson SA, and Emery VJ, 1994: *Strongly Correlated Electronic Materials*, eds. K.S. Bedell et al. (Addison Wesley, Redwood City) p. 619

Mason TE, Aeppli G, Mook HA, 1992: Phys. Rev. Lett. **68**, 1414

Marshall W and Lovesey SM, 1971: *Theory of Thermal neutron Scattering* (Clarendon Press, Oxford)

Matsuda M, Yamada K, Endoh Y, Thurston TR, Shirane G, Birgeneau RJ, Kastner MA, Tanaka I and Kojima H, 1994: Phys. Rev. B **49**, 6958

Nakajima K, Endoh Y, Hosoya S, Wada J, Welz D, Mayer HM, Graf HA and Steiner M, 1996: (submitted)

Samuelsen EJ, Andersen E and Feder J, 1972: *Proceeding of the NATO Advanced Study on Structural Phase Transitions and Soft Modes* (Plenum, New York)

Shirane G, 1959: Acta Cryst. **12**, 282

Shirane G, Uemura YJ, Wicksted JP, Endoh Y and Ishikawa Y, 1985: Phys. Rev. B **31** 1227

Shirane G, Birgeneau RJ, Endoh Y and Kastner MA, 1994: Physica B **197**, 158

Si Q, Zha Y, Levin K and Lu JP, 1993: Phys. Rev. B **47**, 9124

Steinvoll O, Majkrzak CF, Shirane G and Wicksted J, 1984: Phys. Rev. B **30**, 2377

Tanamoto T, Kohno H and Fukuyama H, J.Phys.Soc.Jpn., 1994: **63**, 2739

Tanamoto T, 1995: Thesis, (Univ. Tokyo)

Tokura Y, Urushibara A, Moritomo Y, Arima T, Asamitsu A, Kido G and Furukawa N, 1995: J. Phys. Soc. Jpn. **63**, 3931

Tranquada JM, Steinlieb BJ, Axe JD, Nakamura Y and Uchida S, 1995: Nature **375**, 561

Urushibara A, Moritomo Y, Arima T, Asamitsu A, Kido G and Tokura Y, 1995: Phys. Rev. B **51**, 14103

Wicksted JP, Boni P and Shirane G, 1984: Phys. Rev. B **30** 3655

Wollan EO and Kohler WC, 1955: Phys. Rev. **100**, 545

Yamada K, Endoh Y, Lee CH, Wakimoto S, Arai M, Ubukata K, Fujita M, Hosoya S and Bennington SM, 1994: J. Phys. Soc. Jpn. **64**, 2742

Yamada K, Wakimoto S, Shirane G, Lee CH, Kastner MA, Hosoya S, Greven M, Endoh Y and Birgeneau RJ, 1995: Phys. Rev. Lett. **75**, 1626

Yamada K, Wada J, Kurahashi K, Lee CH, Kimura Y, Wakimoto S, Endoh Y, Hosoya S, Shirane G, Birgeneau RJ and Kastner MA, 1996: (submitted)

Zhang FC and Rice TM, 1988: Phys. Rev. B **37**, 3759